Progress in Nuclear Energy 85 (2015) 17–27

Contents lists available at ScienceDirect

Progress in Nuclear Energy

journal homepage: www.elsevier.com/locate/pnucene

Estimation of relative power distribution and power peaking factor in a VVER-1000 reactor core using artificial neural networks

Ahmad Pirouzmand*, Morteza Kazem Dehdashti

Department of Nuclear Engineering, School of Mechanical Engineering, Shiraz University, Shiraz, Iran

ARTICLE INFO

Article history:
Received 12 February 2015
Received in revised form
28 April 2015
Accepted 1 June 2015
Available online

Keywords:
Real-time monitoring system
Relative power distribution (RPD)
Power peaking factor (PPF)
Artificial neural networks (ANNs)
Ex-core neutron detectors
MCNPX code

ABSTRACT

Designing a computational tool to predict in real-time neutronic parameters of a VVER-1000 reactor core such as axial and radial relative power distributions (RPDs) and power peaking factor (PPF) based on an artificial neural network (ANN) framework is presented in this paper. The method utilizes ex-core neutron detector signals, some core parameters data, and a neural network to setup a real-time monitoring system for RPD and PPF predictions. To detect the hottest fuel assemblies (FAs), the radial RPD in the core is first monitored and then the axial relative power of those FAs is screened to detect the PPF in the core. To achieve this, two hundred reactor operation states with different power density distributions are obtained by positioning the control rods in different configurations. Then a multilayer perceptron (MLP) neural network is trained by applying a set of experimental and calculated data for each core state. The experimental data are core parameters such as control rods position, coolant inlet temperature, power level and signal of ex-core neutron detectors taken from Bushehr nuclear power plant (BNPP) for each operation state. The RPD and PPF for each corresponding state are calculated using a validated model developed in MCNPX 2.7 code. The results of this study indicate that the RPD and PPF can be determined through a neural network having in input the position of control rods, the power level, the coolant inlet temperature, the boric acid concentration, the effective days of reactor operation, and the signal of ex-core neutron detectors, accurately. Also, the sensitivity study of the ANN response to different selection of input parameters illustrates that the signal of ex-core neutron detector plays an important role in the ANN prediction accuracy.

1. Introduction

An accurate prediction on the neutronic parameters of a nuclear reactor core is a major design concept for both economic and safety reasons. Development of economically beneficial and safe operation requires more accurate, comprehensive and real-time analysis of the neutronic parameters (IAEA, 2005). Various safety requirements imposed on the fuel pellets and fuel clad barriers such as the LPD[1] and the DNBR[2] play an important role in protection and monitoring systems. To confirm that these requirements are not violated during the reactor operation a real-time monitoring system is required (Wang et al., 2003). The changes in reactor core power distribution are usually monitored by detecting the neutron flux density via the protection system which uses in-core and ex-core neutron detectors signals. Early monitoring of the reactor power distribution and power peaking factor measurements are performed by miniature fission chamber neutron detectors installed in the in-core instrument channels and the calculation of the power distribution is carried out using a series of neutron flux data. However, utilizing the in-core neutron detectors to compute the power distribution and the other real-time parameters accurately is faced with some difficulties. Core size, high temperature, high pressure and proposing some special materials into the core are limitations of using in-core detectors in some cases (Bae et al., 2009). The purpose of developing an ex-core instrumentation system for advanced reactors, including VVER-1000 reactors, is to increase the safety and efficiency of the nuclear power plant

* Corresponding author.
E-mail address: pirouzm@shirazu.ac.ir (A. Pirouzmand).

[1] Local power density.
[2] Departure from nucleate boiling ratio.

http://dx.doi.org/10.1016/j.pnucene.2015.06.001
0149-1970/

operation by increasing the response speed, reliability and accuracy of the operational monitoring system.

The central objective of this study is to predict the radial and axial RPDs[3] and PPF[4] in a VVER1000 reactor core using measured signals of the reactor coolant system, the ex-core neutron detectors, the power level, and the control rods position. Studying the complex relationship among the power distribution variation, core neutron flux change and the ex-core neutron detector response reveals that artificial neural networks (ANNs[5]) can properly fit the complex nonlinear correlation of these aspects. ANNs allow modeling complex systems without requiring an explicit knowledge or formulation of the relationship that exist among the variables and constitute an alternative to structured models or empirical correlations (Hassoun, 2003). ANNs have been successfully applied to different applications in nuclear engineering from nuclear reactor dynamics simulation to the PPF estimation and the 3D power distribution prediction (Pirouzmand and Hadad, 2011a,b; Hadad and Pirouzmand, 2007; Tanabe and Yamamoto, 1993; Nae et al., 2004; Mary et al., 2006; Montes and Francois, 2009; Xia et al., 2013). This work proposes a method based on the artificial neural network technique to predict the radial and axial RPDs and PPF accurately in real-time. To verify this method, a series of experimental data taken from the Bushehr nuclear power plant (BNPP[6]) are used. All of these parameters are deduced from the core variables such as the signal of ex-core detectors, the position of control rods, the power level, the coolant inlet temperature, and the boric acid concentration.

2. VVER-1000 ex-core nuclear measurement system

Using geometric symmetry, the VVER-1000 reactor core can be segmented into six regions in which each one contain 28 fuel assemblies (FAs[7]). As long as the neutron flux of each segment is obtained, the axial RPD[8] of the core can be calculated in certain conditions. When the reactor core operates at hot zero power each segment can be viewed as a neutron source and the neutron leakage from each segment is almost constant that is monitored by ex-core neutron detectors. The escaped neutrons can cross over the surrounding segments, the reflective layer, and the pressure vessel and finally reach to the ex-core detectors. Meanwhile, the count of the detector is the superposition of the neutrons leaked from each segment. Therefore, a correspondent relationship would exist between the measured data and the neutron flux density value of each segment. In addition, there is a strong correlation for neutron flux between each segment, especially between adjacent ones. Also, the change of the neutron flux in one segment interacts neighboring segments as well as remote segments. The ex-core neutron detector is extremely sensitive to the neutron flux change of the peripheral segment. Consequently, the change of the core neutron flux distribution can be deduced from the count rate of the ex-core neutron detectors (Xia et al., 2013).

The ex-core neutron detectors of the VVER-1000 reactor together with the corresponding electronic systems can monitor the core neutron leakage under power operation within the range of (10^{-9} to 120) % rated power. In addition, the ex-core measurement system provides some critical core parameters such as reactor period over the range of (10–500) seconds, reactivity, monitoring

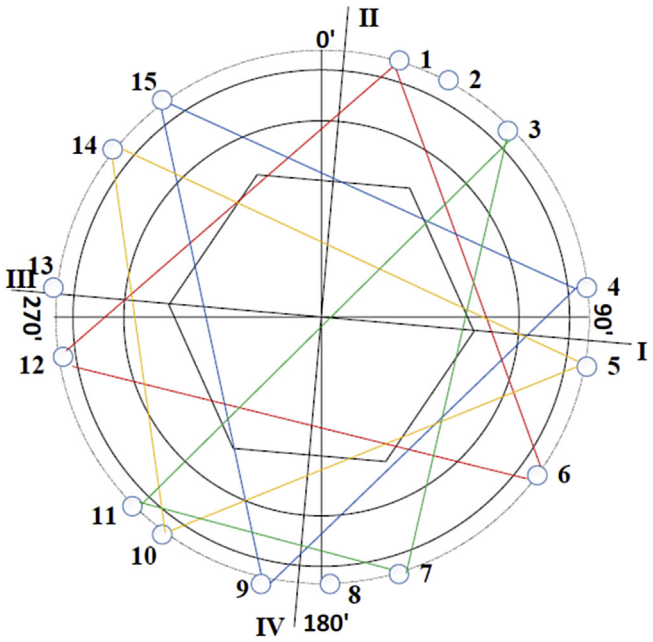

Fig. 1. Diagram of detection unit arrangement in I&C channels (AEOI, 2007).

Table 1
Arrangement of sensors in channels in reactor concrete shield over the core perimeter (AEOI, 2007).

Channel number	Purpose of the channel
1, 6, 12	First set of equipment, start-up and working ranges
4, 9, 15	Second set of equipment, start-up and working ranges
3, 7, 11	First set of equipment, source range
5, 10, 14	Second set of equipment, source range
9	First set of equipment of physical start-up
2, 13	Second set of equipment of physical start-up
13	Redundant channel for equipment of the first set
8	Redundant channel for equipment of the second set

of neutron flux during start-up of reactor and reactor core loading (refueling). Fig. 1 shows the ex-core neutron detectors arrangement around the core in instrumentation and control (I&C[9]) channels. There are provided 15 neutron detector channels in the biological shield with different measuring level. Measuring level is divided into three groups involves start-up, working and source ranges. Table 1 shows the arrangement of sensors in channels in reactor's concrete shield over the core perimeter in two sets of equipment. The detectors are located at different vertical levels. The main task of the ex-core nuclear measurement system is to alarm timely during steady power operation and active the shutdown system when it is needed by monitoring the neutron flux (AEOI, 2007). This research addresses the RPD and PPF predictions from the ex-core measurement system in 1/6 core symmetry. Here, the signal of one neutron detector is used for the neural networks training, validation and testing.

3. MCNPX model

A Monte Carlo method does not solve an explicit equation like a deterministic code; it rather calculates the solutions by simulating

[3] Relative power distributions.
[4] Power peaking factor.
[5] Artificial neural networks.
[6] Bushehr nuclear power plant.
[7] Fuel assemblies.
[8] Relative power distribution.
[9] Instrumentation and control.

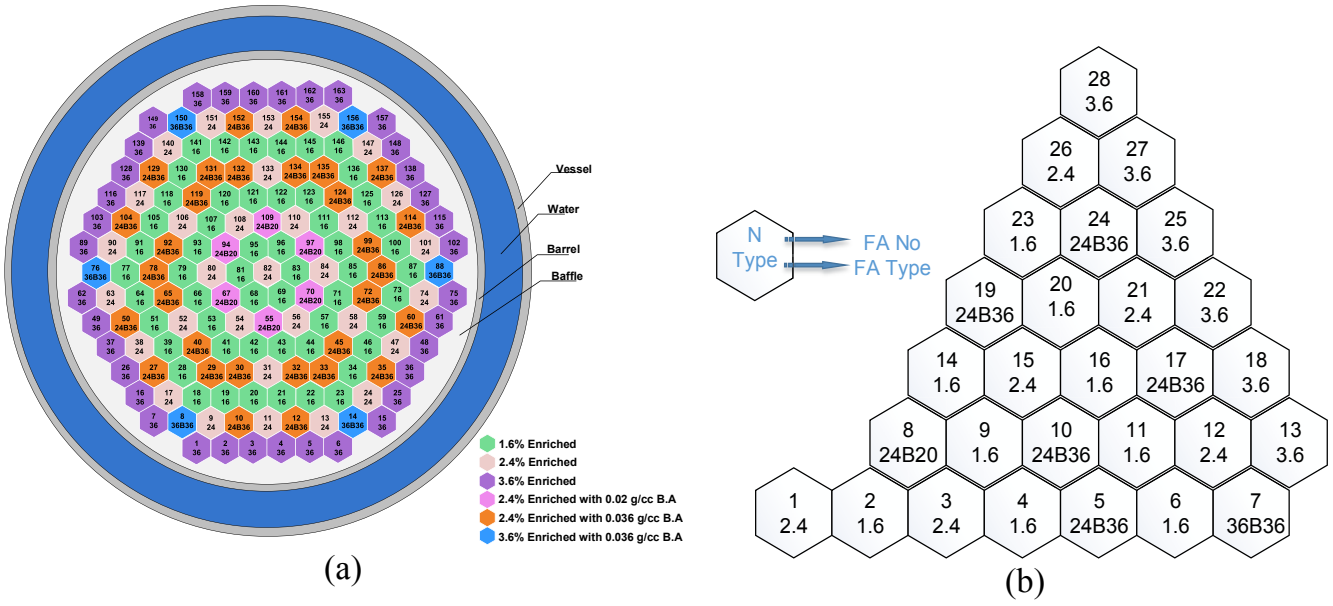

Fig. 2. VVER-1000 core configuration including different FAs in the first fuel cycle (a) whole core and (b) 1/6 core symmetry (AEOI, 2007).

Table 2
Description of FA types used in the first fuel cycle (AEOI, 2007).

FA type	Average enrichment (U_{235}, % weight)	Number of fuel rods type 1 (% enrichment)	Number of fuel rods type 2 (% enrichment)	Number of burnable absorber rods	Boron concentration [g/cm^3]
1.6	1.6	1.6 (311)	–	–	–
2.4	2.4	2.4 (311)	–	–	–
3.6	3.6	3.7 (245)	3.3 (66)	–	–
24B20	2.4	2.4 (311)	–	18	0.020
24B36	2.4	2.4 (311)	–	18	0.036
36B20	3.6	3.7 (245)	3.3 (66)	18	0.020

individual particles and recording some aspects (tallies) of their average behavior. Monte Carlo codes make use of a continuous energy scale to represent the variation of the cross section data that are widely used because of their capability in modeling of complex geometries (Dunn and Shultis, 2011). MCNPX 2.7 which is a Monte Carlo based computer code and has some features such as being general-purpose, continuous-energy, generalized-geometry, burnup calculation capability, and various particle transport calculation is used in this research for RPD and PPF calculations (Briemeister, 2013).

Table 3
The calculated MCNPX model results compared with BNPPNA data.

T_{eff} [day]	T_{in} [°C]	H10 [%]	P [MW]	C_{bc} [g/kg]	BNPPNA (AEOI, 2004)					MCNPX model				
					K_q		K_v			K_q		K_v		
					[relative]	[N_k]	[relative]	[N_k]	[N_z]	[relative]	[N_k]	[relative]	[N_k]	[N_z]
0.0	280.5	60	150	6.83	1.42	25	2.07	25	5	1.42	25	2.07	25	5
1.0	282.8	60	750	6.04	1.34	21	1.90	21	4	1.34	21	1.90	21	4
5.0	284.4	70	1200	5.60	1.29	21	1.78	21	5	1.29	21	1.78	21	5
10.0	285.5	80	1500	5.36	1.26	21	1.71	21	5	1.26	21	1.71	21	5
15.0	285.5	80	1500	5.30	1.26	21	1.69	21	5	1.25	21	1.67	21	5
20.0	288.3	80	2250	4.95	1.22	21	1.66	21	4	1.22	21	1.66	21	4
40.0	288.3	80	2250	4.74	1.22	1	1.60	1	5	1.22	1	1.60	1	5
60.0	288.3	80	2250	4.16	1.22	1	1.52	3	5	1.22	1	1.52	3	5
70.0	288.3	80	2700	3.93	1.24	1	1.52	3	4	1.23	1	1.50	3	4
80.0	291.0	90	3000	3.93	1.24	1	1.45	3	4	1.24	1	1.44	3	4
100.0	291.0	90	3000	3.58	1.22	3	1.39	3	3	1.21	3	1.39	3	3
120.0	291.0	90	3000	2.23	1.21	3	1.37	3	3	1.21	3	1.35	3	3
160.0	291.0	90	3000	2.51	1.19	3	1.32	3	3	1.18	3	1.32	3	3
200.0	291.0	90	3000	1.76	1.17	3	1.31	3	2	1.17	3	1.31	3	2
240.0	291.0	90	3000	1.01	1.15	3	1.31	15	2	1.15	3	1.31	15	2
260.0	291.0	90	3000	0.63	1.15	3	1.31	15	2	1.14	3	1.31	15	2
293.0	291.0	90	3000	0.00	1.14	3	1.30	15	2	1.14	3	1.30	15	2
293.8	291.0	90	3000	0.00	1.14	3	1.30	15	2	1.14	3	1.29	15	2

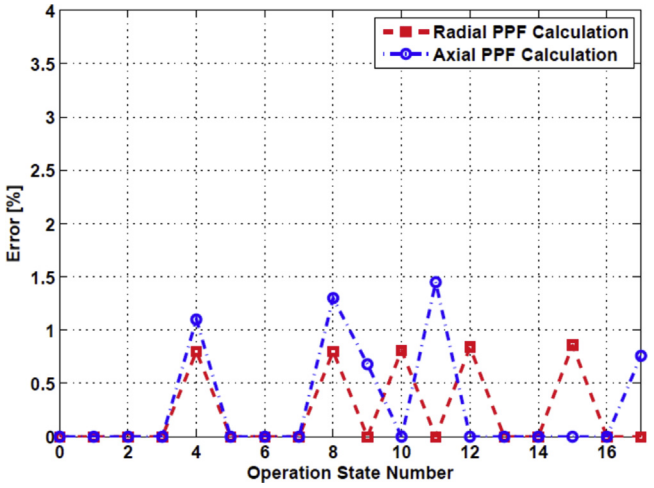

Fig. 3. Calculated average error of MCNPX model results for all operation states given in Table 2.

In this study, a VVER-1000 reactor core model is designed and developed by MCNPX 2.7 code. The model contains all physical core components in real reactor operation conditions. The RPD and PPF are calculated using tally type F4 of MCNPX together with FM and SD cards. An accurate MCNP model is accomplished in a step by step procedure by considering all factors that affect the RPD and PPF calculations. In this model, the reactor core geometry which covers all fuel rods (fuel, gap and clad), burnable absorber rods, water channels, guide channels, control rods, baffle, and vessel is considered in details. Moreover, the reactor core is segmented axially into 10 equally spaced zones to study the effect of temperature profile and density variations in axial direction on core material atom density calculations and cross section data libraries generation (Doppler Effect). The temperature profiles of coolant and fuel material are obtained by a verified model of VVER-1000 reactor based on Unit 1 of BNPP developed in RELAP5/MOD3.2 code. The RELAP5 model consists of 4-loop primary and secondary systems with all their relevant sub-systems (Pirouzmand et al., 2014). The effect of S (alpha, beta) thermal scattering and the temperature influence on its value is also considered. The cross sections and thermal scattering of each axial zone in the mean temperatures are produced by *makxsf* module provided in the MCNPX code. The makxsf is a utility program for manipulating cross-section library files of the MCNP5 Monte Carlo code. Routines from the NJOY and DOPPLER codes were incorporated into makxsf to provide Doppler broadening of resolved data to any higher temperature (Brown, 2000). The control rods movements, burnup effect with axial variation in the core, and the effect of fission products on the neutron flux are also modeled. All simulations are carried out with high number of histories by a computer cluster system using message passing interface (MPI[10]) parallelization.

The RPD is affected by major factors such as: the time of operation, the coolant inlet temperature, the position of control rods groups, the power level, and the boric acid concentration. Fig. 2 shows BNPP VVER-1000 core configuration including different FAs with corresponding enrichment value at the first fuel cycle. The characteristics of different FA types used at the first fuel cycle are tabulated in Table 2 (AEOI, 2007).

[10] Message passing interface.

The MCNPX model is validated against BNPP final safety analysis report (FSAR[11]) and neutron album data during the first fuel cycle. The calculation is carried out in the first fuel cycle for 0.00–293.82 days of operation with variation in the control rods position, the boric acid concentration, the power level, and the coolant inlet temperature. Also, many actual steady operation states with different effective factors are applied to calculate the axial and radial RPDs for each FA in ten axial nodes. Table 3 presents some of the MCNPX model results which are compared to the BNPP neutron album (BNPPNA[12]) data. In this table T_{eff}, T_{in}, H10, P, C_{bc}, K_q, K_v, N_k, and N_z are the time of reactor operation, the core inlet temperature, the position of control rods group 10 (percent of withdrawn length), the power level, the boric acid concentration, the radial and axial PPFs, FA[13] number, and the core axial level, respectively. The calculated radial and axial RPDs and PPF using MCNPX model are compared to the BNPPNA data for all states given in Table 3. As shown there is a good comparison between the MCNPX model and the BNPPNA data for K_q and K_v calculations and their location in the core. The calculated average error of MCNPX model results for all operation states are shown in Fig. 3. The maximum error is less than 1.5% and 1% for axial and radial data, respectively, which is accurate enough to be used in the RPD monitoring.

Also, Fig. 4 illustrates the radial and axial RPDs for an operation state with reactor core parameters given in Table 4 for further comparison. As shown there is a very good comparison between the MCNPX model results and BNPPNA data. In this table H8, H9 and Si_{ex} are the position of group 8 and 9 of control rods and the signal of ex-core neutron detector, respectively.

4. Training data

In this research, 200 reactor operation states with different power density distributions are considered and a database is prepared. The database is composed of about 58,000 different data holding axial and radial relative power distributions for 1/6 reactor core symmetry along some reactor core physical parameters. The database is divided into three categories: The first subset consists of the first fuel cycle core operation states from cold zero power to hot full power with considering the change in the coolant inlet temperature, the power level, the position of control rods of group 10, the boric acid concentration, the magnitude of ex-core detector signal and the corresponding axial and radial RPDs and PPF calculated using the MCNPX model. The second subset covers reactor core shutdown states including all mentioned core parameters and especially changes in reactor controlling parameters. This time, the position of three control rods groups is altered (H10 from 100 to 0, H9 from 100 to 6.6, and H8 from 100 to 66.6 percent). In the second category, the correlation between changing the position of control rods groups and the relative power magnitude is more observable. The third group is related to miscellaneous circumstances which encloses the irregular change in the position of three control rods groups, the boric acid concentration, and the power level during different effective days of operation along with the MCNPX model output data and the signal of ex-core detector. Table 5 shows some of reactor core operation states in the above three mentioned categories.

[11] Final safety analysis report.
[12] Bushehr nuclear power plant neutron album.
[13] Fuel assembly.

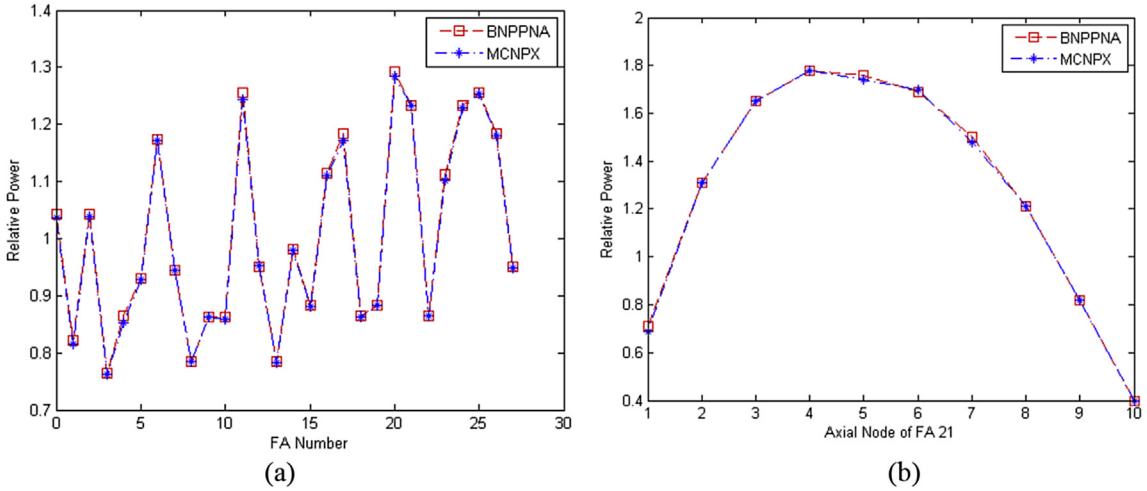

Fig. 4. Comparison of the MCNPX model results with BNPP neutron album data (a) radial and (b) axial relative power for the operation state given in Table 3.

Table 4
One of reactor operation state investigated for MCNPX model validation.

Reactor core parameter	Si_{ex} [A]	H8 [%]	H9 [%]	H10 [%]	C_{bc} [g/kg]	T_{in} [°C]	P [MW]	T_{eff} [day]
Value	8.23E-05	100	100	70	5.60	284.4	1200	5.0

Table 5
Samples of reactor operation states used in the training process.

Reactor core parameters								
	H10 [%]	H9 [%]	H8 [%]	T_{eff} [day]	T_{in} [°C]	P [MW]	C_{bc} [g/kg]	Si_{ex} [A]
Start-up and steady state operation	90.0	100.0	100.0	120.0	291.0	100	3.23	1.42E-4
	90.0	100.0	100.0	140.0	291.0	100	2.87	1.42E-4
	90.0	100.0	100.0	160.0	291.0	100	2.51	1.42E-4
	90.0	100.0	100.0	180.0	291.0	100	2.14	1.42E-4
	90.0	100.0	100.0	200.0	291.0	100	1.76	1.42E-4
	90.0	100.0	100.0	220.0	291.0	100	1.39	1.42E-4
	90.0	100.0	100.0	240.0	291.0	100	1.01	1.42E-4
	90.0	100.0	100.0	260.0	291.0	100	0.63	1.42E-4
	90.0	100.0	100.0	280.0	291.0	100	0.26	1.42E-4
	90.0	100.0	100.0	293.8	291.0	100	0.00	1.42E-4
Shut-down(trip in day 100.0)	90.0	100.0	100.0	100.0	291.0	100	3.58	1.42E-4
	76.6	100.0	100.0	100.0	289.9	90	3.58	1.40E-4
	63.3	100.0	100.0	100.0	288.8	80	3.58	1.40E-4
	50.0	100.0	100.0	100.0	287.7	70	3.58	1.40E-4
	36.6	96.6	100.0	100.0	286.6	60	3.58	1.40E-4
	23.3	83.3	100.0	100.0	285.5	50	3.58	1.40E-4
	16.6	76.6	100.0	100.0	284.4	40	3.58	1.40E-4
	6.6	66.6	100.0	100.0	283.3	30	3.58	1.40E-4
	0.0	56.6	100.0	100.0	282.2	20	3.58	1.40E-4
	0.0	43.3	100.0	100.0	281.1	10	3.58	1.40E-4
Miscellaneous circumstances	0.0	0.0	60.0	5.0	291.0	40	4.69	1.40E-4
	0.0	0.0	50.0	5.0	291.0	40	4.60	8.25E-5
	0.0	0.0	40.0	5.0	291.0	40	4.50	8.25E-5
	0.0	0.0	30.0	5.0	291.0	40	4.37	8.25E-5
	0.0	0.0	20.0	5.0	291.0	40	4.23	8.25E-5
	0.0	0.0	10.0	5.0	291.0	40	4.13	8.25E-5
	0.0	0.0	0.0	5.0	291.0	40	4.09	8.25E-5
	30.0	90.0	100	50.0	291.0	75	4.65	9.90E-5
	20.0	80.0	100	50.0	291.0	75	4.65	9.90E-5
	10.0	70.0	100	50.0	291.0	75	4.65	9.90E-5

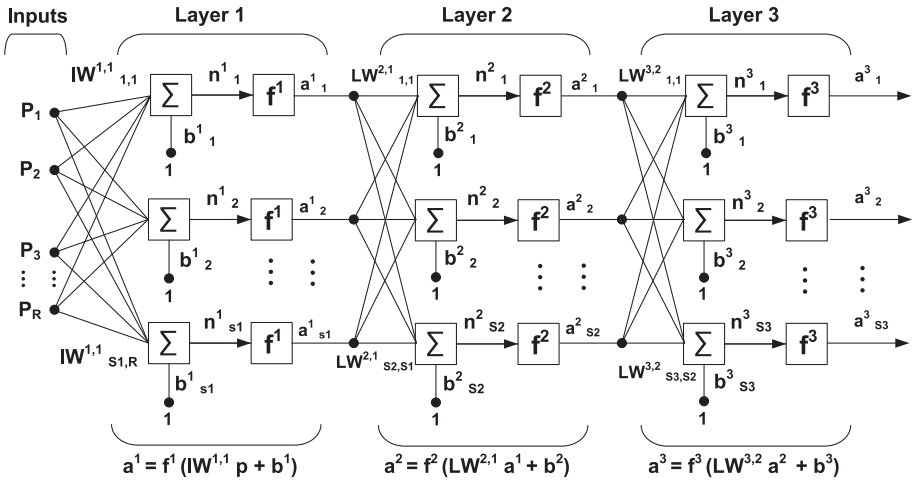

Fig. 5. Multi-layer perceptron neural network structure (Hassoun, 2003).

Table 6
Architecture and root mean square error for proposed MLP neural networks.

	Architecture (# of neuron in each hidden layer)	MSE	Regression fraction
Case 1	(5)	0.0111	0.9374
Case 2	(3,10)	0.0095	0.9337
Case 3	(7,10)	0.0052	0.9276
Case 4	(9,10)	0.0009	0.9827
Case 5	(13,10)	0.0029	0.9789

5. Artificial neural networks

Artificial neural networks (ANNs) are defined as a parallel distributed processor consisting of a great number of processing elements, known as neurons, connected to each other with different connection strengths. The strength of a connection between neurons is called weight. In beginning of a neural network development process, these weights are initialized randomly and

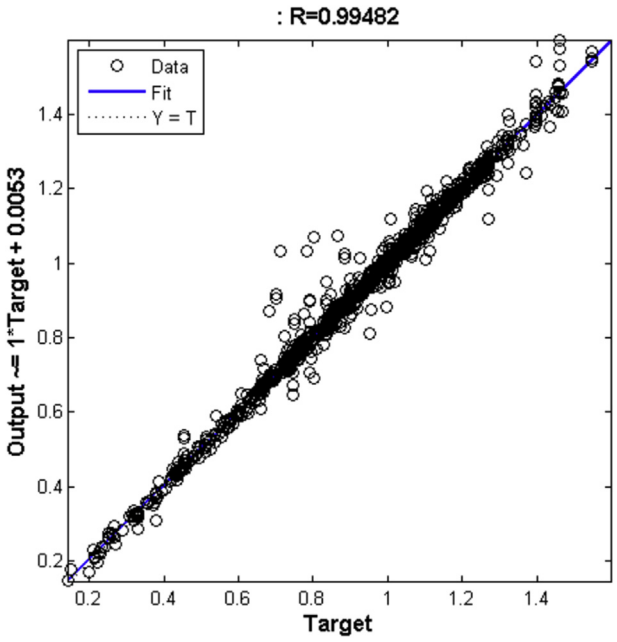

Fig. 7. Regression plot for total data.

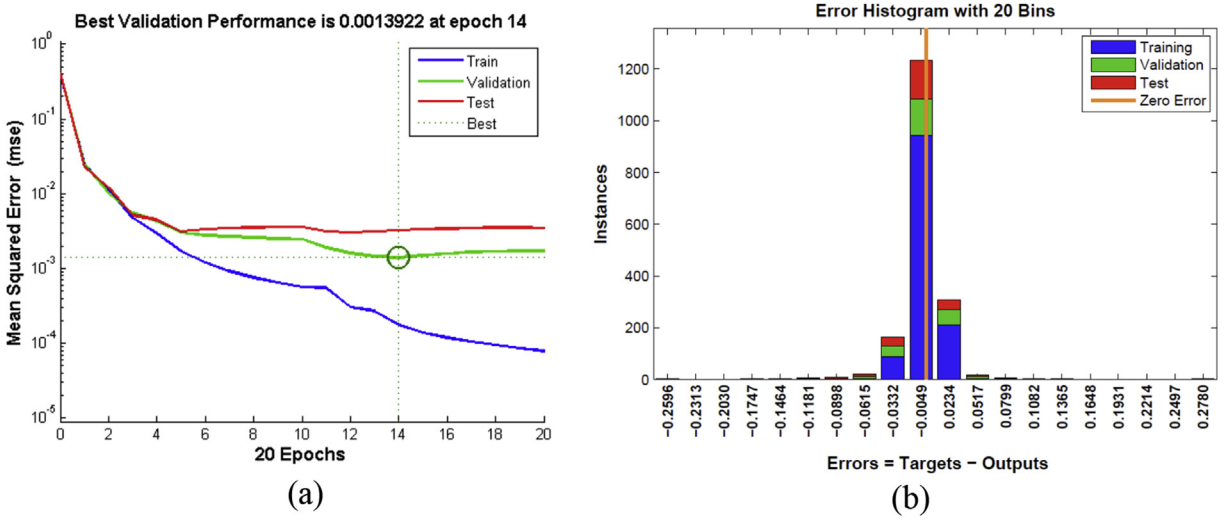

Fig. 6. The performance of MPL network during training, validation, and testing processes: (a) MSE (b) error aggregation.

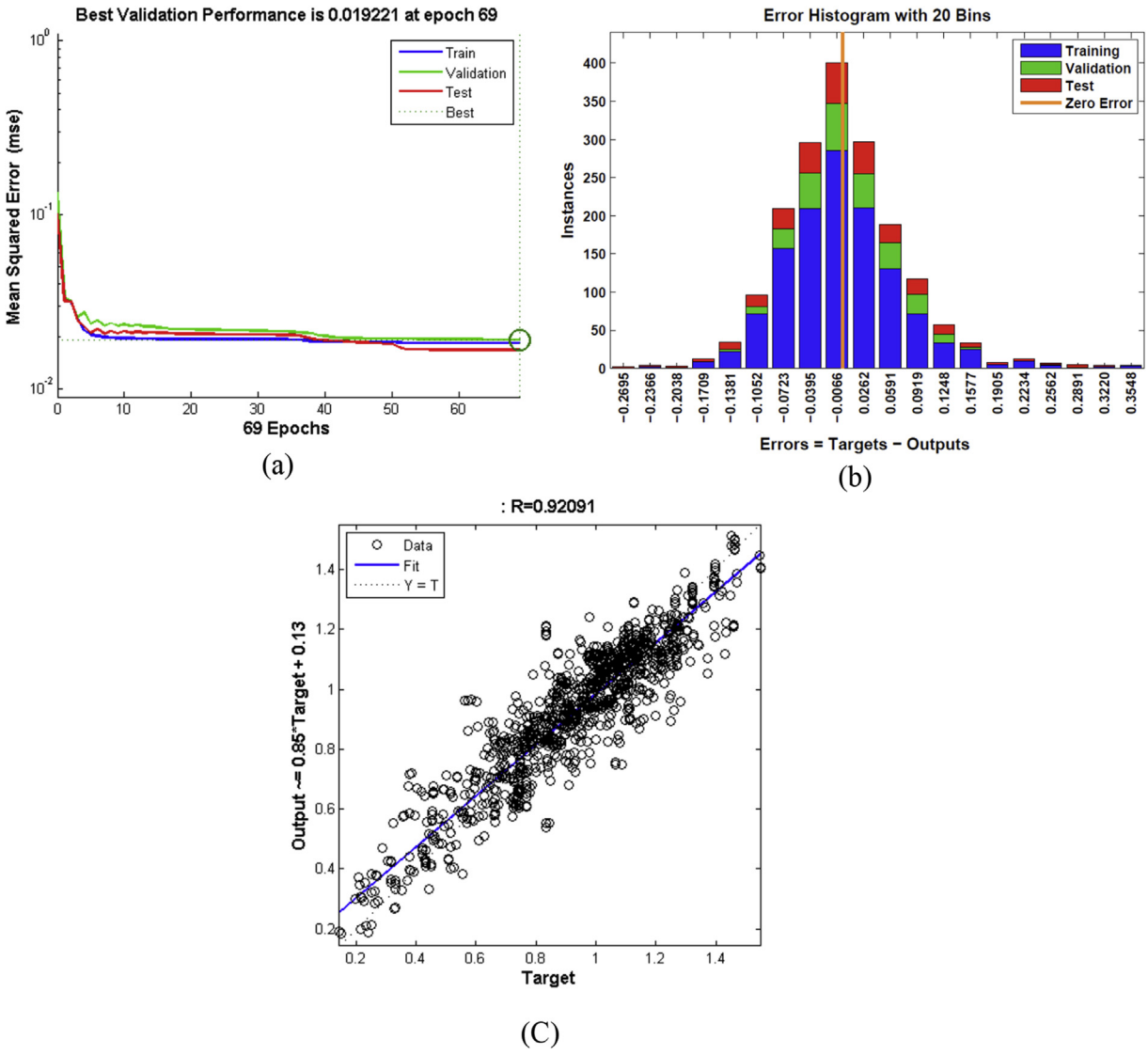

Fig. 8. The performance of MPL network after omitting the ex-core detector signal from the input vector: (a) MSE (b) Error aggregation (c) Regression plot for total data.

adjusted in a network training process in a way that it minimizes the error between the calculated and the corresponding target output values for a particular training data set and a testing subset is used to check the performance of the developed network. There are different type of ANNs depending on their applications. Fig. 5 shows the structure of a multi-layer perceptron (MLP[14]) neural network with three hidden layers used in this study (Hassoun, 2003).

Two hundred samples from the MCNPX model and experimental data are used to train, validate and test the networks. The RPDs and PPF could be correlated to several variables. These variables and relative power distributions can be utilized for training and validating the neural networks. According to variables slection, the input vectors could be different. Herein, the input vector includes the signal of ex-core detector (Si_{ex}), the position of control rods for group 8, 9, and 10 (H8, H9, and H10), the coolant inlet temperature (T_i), the effective day of reactor operation (T_{eff}), the

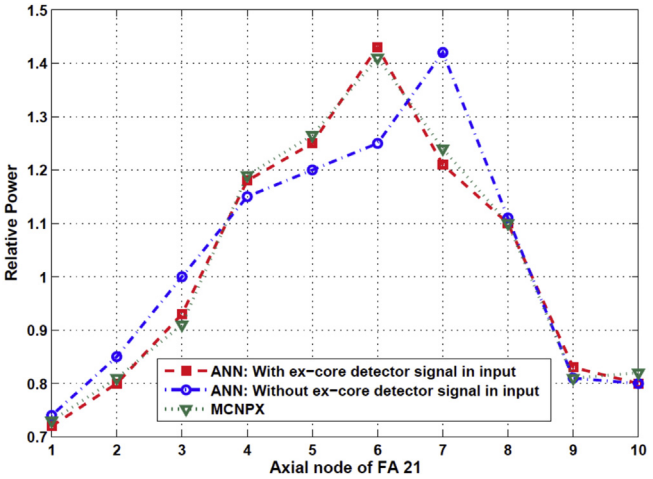

Fig. 9. Axial relative power estimation using the MLP networks with and without the ex-core detector signal in the input vector compared to the MCNPX model data.

[14] multi-layer perceptron.

Table 7
Five reactor operation states used for the network performance evaluation of axial and radial RPDs prediction.

Core parameter	Si_{ex} [A]	H8 [%]	H9 [%]	H10 [%]	C_{bc} [g/kg]	Ti [°C]	P [MW]	T_{eff} [day]
Case 1	8.23E-05	100.0	100.0	70.0	5.60	284.4	1200	5.0
Case 2	8.25E-05	30.0	90.0	0.0	4.99	284.4	1200	5.0
Case 3	3.43E-04	100.0	70.0	10.0	–	284.4	1500	200.0
Case 4	3.85E-04	100.0	66.6	6.6	–	283.3	1250	100.0
Case 5	2.65E-03	10.0	80.0	20.0	–	281.0	500	300.0

Table 8
RPD prediction by ANN compared to BNPPNA data for Case 1 given in Table 7.

		Axial node's number in each FA									
			1	2	3	4	5	6	7	8	9	10
FA's number	1	BNPPNA	0.56	1.02	1.30	1.43	1.45	1.39	1.24	1.00	0.71	0.35
		ANN	0.55	1.00	1.30	1.43	1.44	1.39	1.23	1.00	0.71	0.34
	2	BNPPNA	0.45	0.80	1.02	1.13	1.15	1.10	0.98	0.79	0.55	0.28
		ANN	0.43	0.80	1.02	1.13	1.15	1.09	0.98	0.79	0.55	0.25
	3	BNPPNA	0.57	1.03	1.31	1.44	1.46	1.39	1.23	0.97	0.67	0.33
		ANN	0.55	1.03	1.31	1.43	1.46	1.39	1.21	0.97	0.67	0.30
	4	BNPPNA	0.42	0.75	0.95	1.05	1.07	1.02	0.89	0.70	0.48	0.24
		ANN	0.41	0.75	0.93	1.04	1.07	1.02	0.83	0.70	0.48	0.22
	5	BNPPNA	0.48	0.86	1.09	1.19	1.21	1.15	1.02	0.81	0.57	0.28
		ANN	0.44	0.86	1.07	1.19	1.20	1.13	1.02	0.80	0.57	0.27
	6	BNPPNA	0.51	0.92	1.15	1.26	1.27	1.20	1.08	0.88	0.63	0.32
		ANN	0.53	0.90	1.15	1.24	1.27	1.17	1.08	0.88	0.61	0.31
	7	BNPPNA	0.64	1.18	1.48	1.60	1.60	1.51	1.35	1.12	0.81	0.39
		ANN	0.61	1.18	1.48	1.58	1.60	1.50	1.35	1.11	0.81	0.38
	8	BNPPNA	0.51	0.93	1.17	1.29	1.32	1.25	1.11	0.88	0.61	0.30
		ANN	0.50	0.93	1.14	1.29	1.31	1.25	1.11	0.87	0.60	0.30
	9	BNPPNA	0.44	0.79	1.00	1.10	1.12	1.06	0.93	0.70	0.47	0.23
		ANN	0.45	0.77	1.00	1.10	1.11	1.06	0.92	0.70	0.47	0.21
	10	BNPPNA	0.49	0.87	1.10	1.21	1.23	1.17	1.02	0.77	0.52	0.26
		ANN	0.42	0.85	1.10	1.21	1.22	1.15	1.02	0.77	0.50	0.25
	11	BNPPNA	0.48	0.86	1.09	1.19	1.20	1.14	1.01	0.82	0.58	0.29
		ANN	0.48	0.85	1.09	1.18	1.20	1.14	1.01	0.80	0.58	0.29
	12	BNPPNA	0.69	1.27	1.58	1.71	1.71	1.62	1.45	1.19	0.86	0.42
		ANN	0.69	1.24	1.58	1.70	1.71	1.62	1.45	1.19	0.85	0.40
	13	BNPPNA	0.51	0.97	1.21	1.30	1.30	1.23	1.10	0.91	0.66	0.32
		ANN	0.51	0.96	1.21	1.27	1.30	1.21	1.10	0.90	0.65	0.32
	14	BNPPNA	0.44	0.79	1.00	1.10	1.12	1.06	0.93	0.70	0.47	0.23
		ANN	0.44	0.77	1.00	1.10	1.12	1.06	0.91	0.70	0.45	0.22
	15	BNPPNA	0.58	1.05	1.32	1.45	1.47	1.39	1.15	0.75	0.44	0.21
		ANN	0.55	1.05	1.32	1.45	1.45	1.39	1.14	0.75	0.43	0.21
	16	BNPPNA	0.50	0.89	1.12	1.23	1.24	1.17	1.03	0.79	0.54	0.27
		ANN	0.52	0.89	1.12	1.23	1.24	1.15	1.03	0.77	0.54	0.25
	17	BNPPNA	0.62	1.13	1.41	1.53	1.53	1.45	1.29	1.05	0.75	0.37
		ANN	0.62	1.13	1.40	1.53	1.53	1.45	1.27	1.05	0.75	0.37
	18	BNPPNA	0.64	1.21	1.50	1.62	1.61	1.52	1.36	1.12	0.81	0.39
		ANN	0.64	1.21	1.50	1.62	1.61	1.50	1.36	1.12	0.81	0.38
	19	BNPPNA	0.49	0.87	1.10	1.21	1.23	1.17	1.02	0.77	0.52	0.26
		ANN	0.48	0.87	1.10	1.21	1.23	1.16	1.02	0.77	0.52	0.25
	20	BNPPNA	0.50	0.89	1.12	1.23	1.24	1.17	1.03	0.79	0.54	0.27
		ANN	0.50	0.84	1.12	1.23	1.24	1.16	1.03	0.79	0.54	0.26
	21	BNPPNA	0.72	1.32	1.65	1.77	1.78	1.69	1.50	1.21	0.86	0.42
		ANN	0.72	1.32	1.64	1.76	1.78	1.65	1.50	1.20	0.86	0.42
	22	BNPPNA	0.67	1.26	1.57	1.69	1.68	1.59	1.42	1.16	0.84	0.40
		ANN	0.67	1.25	1.57	1.69	1.67	1.59	1.42	1.16	0.83	0.40
	23	BNPPNA	0.48	0.86	1.09	1.19	1.20	1.14	1.01	0.82	0.58	0.29
		ANN	0.47	0.86	1.09	1.18	1.20	1.14	1.01	0.82	0.57	0.29
	24	BNPPNA	0.62	1.13	1.41	1.53	1.53	1.45	1.29	1.05	0.75	0.37
		ANN	0.60	1.13	1.41	1.53	1.53	1.44	1.29	1.05	0.75	0.36
	25	BNPPNA	0.67	1.26	1.57	1.69	1.68	1.59	1.42	1.16	0.84	0.40
		ANN	0.67	1.26	1.56	1.69	1.68	1.59	1.42	1.16	0.83	0.40
	26	BNPPNA	0.69	1.27	1.58	1.71	1.71	1.62	1.45	1.19	0.86	0.42
		ANN	0.68	1.27	1.57	1.71	1.71	1.62	1.45	1.18	0.86	0.42
	27	BNPPNA	0.64	1.21	1.50	1.62	1.61	1.52	1.36	1.12	0.81	0.39
		ANN	0.64	1.20	1.50	1.62	1.61	1.51	1.36	1.12	0.81	0.39
	28	BNPPNA	0.51	0.97	1.21	1.30	1.30	1.23	1.10	0.91	0.66	0.32
		ANN	0.50	0.95	1.20	1.30	1.30	1.22	1.10	0.91	0.66	0.32

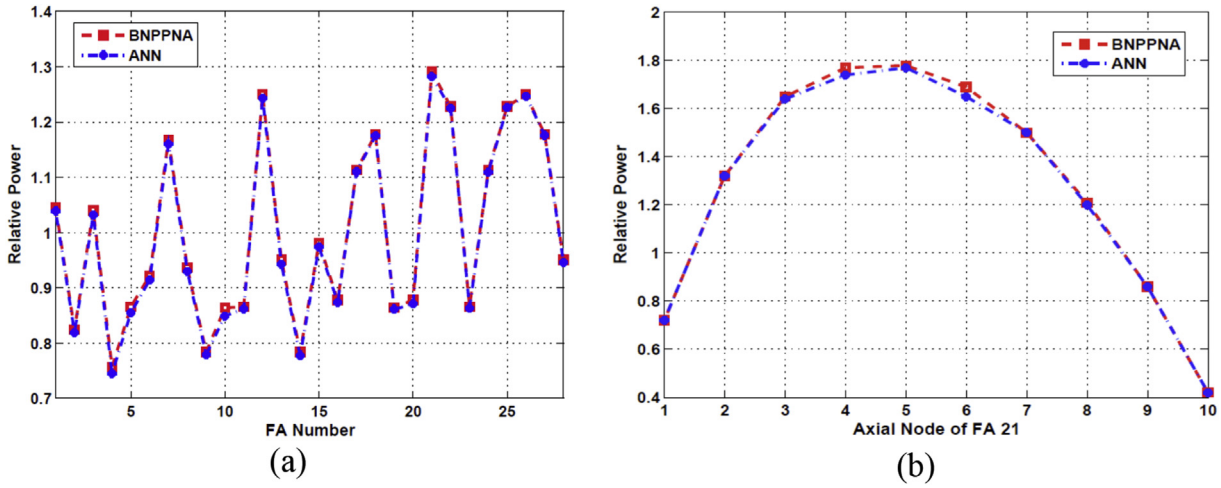

Fig. 10. ANN prediction results for Case 1 compared to BNPPNA data (a) radial RPD and (b) axial RPD in FA number 21.

boric acid concentration (C_{bc}) and the power level (P). The outputs of network are the radial relative power for 28 FAs and axial relative power in ten axial layers for each FA.

The database is divided into two files to train the network. An input file that includes a matrix with 200 rows and 10 columns in which each row contains the reactor core parameters and the ex-core neutron detector signal for a given state. The target file is a 200 × 280 matrix covering the relative power at ten axial nodes of each FA in 1/6 core symmetry (28 FAs).

In this study, MLP neural networks with one and two hidden layers with various number of neuron in each layer are investigated to choose the best network architecture. The MLP networks are model in MATLAB Neural Network Toolbox. *Logsig* and *Purelin* transformation functions are utilized and the train function in this work is *trainlm* which is a network training function that updates weight and bias values according to Levenberg-Marquardt optimization algorithm (Beale et al., 2014). Seventy percent of the data sets is used for training, 15% is applied for validation and the remaining 15% is employed to test the proposed networks. The performance of networks to estimate the RPD is summarized in Table 6. This table shows the topologies and the calculated mean square error (MSE[15]) during the training process. In the training stage, the initial weight and bias values that give the minimum error are found for each neural network after trying more than fifty different randomly selected initial weights and biases.

For the MLP neural networks, the average MSE is 0.00592. The minimum MSE is 0.000923 which is for Case 4, therefore for further investigation Case 4 is chosen. The chosen MPL neural network (Case 4) contains10 and 9 neurons in hidden layers. The magnitude of error for training, validation and testing are 0.000923, 0.0081, and 0.00981, respectively. Fig. 6 shows the aggregation of network's error in the training, validation and testing processes. The error aggregation is observed to occur around the minimum error which is a criterion for a neural network with the efficient performance. The best performance of the network takes place in 14 epochs as illustrated in Fig. 6.

Another step in validating the network is to create a regression plot which shows the relationship between the outputs of the network and the targets. If the training were perfect, the network outputs and the targets would be exactly equal, but the relationship is rarely perfect in practice. For Case 4 MPL network, a regression plot as shown in Fig. 7 that represent the regression plot for total data (training, validation and testing) is plotted. The solid line represents the best fit linear regression line between outputs and targets. The R value is an indication of the relationship between the outputs and targets. If R = 1, this indicates that there is an exact linear relationship between outputs and targets. If R is close to zero, then there is no linear relationship between outputs and targets. In our case, the training data indicates a good fit. The validation and test results also show R values that are greater than 0.99.

As mentioned before different network's input vectors could be considered based on the number of selected core parameters. Investigation of different core parameters used in training process shows that the neutron flux change is extremely sensitive to the position of control rods groups and the ex-core neutron detector signal. Therefore, in the following to express the importance of ex-core neutron detector signal's role in the network response, the ex-core signal is omitted from all input data in the network training process. The MSE value and the error aggregation plots reveal that the network performance is getting worst (Fig. 8). Also the network regression fraction reduces to 0.92. Furthermore, as shown in Fig. 9, the network output (RPD) illustrates a shift in the maximum of axial relative power estimation in comparison with another network having the ex-core detector signal as an input.

6. ANN prediction results

In this section the real-time prediction of relative power distribution and power peaking factor by the MLP network and a comparison with the BNPPNA data are discussed for five core states presented in Table 7 which are not used in training, validation, and testing processes. Table 8 presents the RPD prediction in 1/6 core by the ANN compared to BNPPNA data for Case 1 core operation state given in Table 7. The PPF is occurred in the fifth node of FA number 21 where the neural network predicts the value of power peaking factor with 0.56% error. These data are also plotted in Fig. 10(a) and (b) for graphical comparison. Fig. 10(a) illustrates the radial RPD prediction for 1/6 core symmetry (28 FAs) compared to BNPPNA data and Fig. 10(b) shows the axial RPD prediction in FA number 21 where the PPF is occurred. Same data as Table 7 but for Case 2 is presented in Table 9. In this case the PPF is occurred in the third node of FA number 27 where the neural network predicts the value of PPF with 0.6% error. Fig. 11(a) illustrates the radial RPD prediction for 1/6 core symmetry compared to BNPPNA data and Fig. 11(b)

[15] Mean square error.

Table 9
RPD prediction by ANN compared with BNPPNA data for Case 2 given in Table 7.

			Axial node's number in each FA									
			1	2	3	4	5	6	7	8	9	10
FA's number	1	BNPPNA	0.75	0.97	1.18	1.12	0.93	0.77	0.64	0.57	0.38	0.14
		ANN	0.71	0.97	1.14	1.12	0.93	0.76	0.64	0.57	0.37	0.14
	2	BNPPNA	0.77	1.01	1.20	1.15	0.93	0.77	0.64	0.59	0.35	0.15
		ANN	0.77	1.01	1.21	1.15	0.93	0.77	0.64	0.59	0.33	0.16
	3	BNPPNA	1.02	1.32	1.58	1.50	1.26	1.02	0.86	0.72	0.51	0.20
		ANN	1.06	1.32	1.58	1.50	1.26	1.02	0.85	0.72	0.51	0.21
	4	BNPPNA	0.74	0.96	1.16	1.07	0.92	0.73	0.63	0.54	0.37	0.17
		ANN	0.74	0.96	1.16	1.05	0.92	0.73	0.63	0.54	0.36	0.17
	5	BNPPNA	0.82	1.04	1.27	1.19	1.02	0.80	0.69	0.68	0.45	0.15
		ANN	0.82	1.04	1.26	1.19	1.02	0.81	0.69	0.66	0.45	0.16
	6	BNPPNA	0.72	0.93	1.12	1.06	0.89	0.71	0.61	0.55	0.36	0.14
		ANN	0.72	0.93	1.12	1.06	0.89	0.71	0.60	0.55	0.36	0.13
	7	BNPPNA	1.18	1.53	1.84	1.73	1.46	1.16	0.99	0.89	0.59	0.23
		ANN	1.18	1.52	1.84	1.73	1.46	1.16	0.99	0.88	0.59	0.23
	8	BNPPNA	0.78	1.01	1.22	1.15	0.97	0.77	0.66	0.59	0.39	0.15
		ANN	0.78	1.03	1.22	1.15	0.97	0.77	0.66	0.59	0.38	0.15
	9	BNPPNA	0.92	1.20	1.44	1.36	1.14	0.91	0.78	0.71	0.47	0.18
		ANN	0.92	1.21	1.44	1.36	1.13	0.91	0.77	0.73	0.47	0.17
	10	BNPPNA	0.73	0.95	1.14	1.07	0.91	0.72	0.62	0.55	0.37	0.14
		ANN	0.70	0.95	1.14	1.07	0.91	0.71	0.62	0.55	0.37	0.14
	11	BNPPNA	0.80	1.04	1.24	1.17	1.00	0.76	0.68	0.63	0.40	0.15
		ANN	0.81	1.03	1.24	1.17	1.02	0.76	0.68	0.63	0.42	0.15
	12	BNPPNA	0.84	1.12	1.35	1.27	1.07	0.85	0.72	0.65	0.44	0.17
		ANN	0.84	1.12	1.34	1.27	1.07	0.85	0.72	0.65	0.44	0.17
	13	BNPPNA	1.30	1.69	2.03	1.91	1.61	1.28	1.10	0.99	0.66	0.25
		ANN	1.35	1.69	2.03	1.91	1.61	1.28	1.11	0.99	0.66	0.25
	14	BNPPNA	1.03	1.34	1.61	1.53	1.29	1.02	0.87	0.79	0.52	0.19
		ANN	1.03	1.34	1.61	1.53	1.29	1.02	0.87	0.79	0.52	0.19
	15	BNPPNA	0.92	1.20	1.42	1.36	1.16	0.94	0.78	0.70	0.47	0.18
		ANN	0.92	1.20	1.42	1.36	1.16	0.94	0.78	0.69	0.47	0.18
	16	BNPPNA	1.04	1.36	1.63	1.53	1.30	1.03	0.88	0.72	0.53	0.20
		ANN	1.04	1.36	1.63	1.53	1.31	1.03	0.88	0.72	0.53	0.20
	17	BNPPNA	0.73	0.95	1.14	1.07	0.90	0.72	0.61	0.55	0.37	0.15
		ANN	0.73	0.95	1.14	1.07	0.90	0.72	0.61	0.55	0.37	0.15
	18	BNPPNA	0.61	0.82	1.04	0.99	0.83	0.66	0.57	0.50	0.34	0.13
		ANN	0.61	0.82	1.04	0.99	0.83	0.66	0.57	0.51	0.34	0.13
	19	BNPPNA	0.85	1.18	1.36	1.27	1.08	0.85	0.74	0.63	0.43	0.17
		ANN	0.85	1.18	1.36	1.27	1.08	0.85	0.74	0.63	0.43	0.17
	20	BNPPNA	1.23	1.59	1.92	1.81	1.56	1.21	1.06	0.93	0.66	0.24
		ANN	1.23	1.58	1.92	1.81	1.56	1.21	1.06	0.93	0.66	0.23
	21	BNPPNA	1.32	1.73	2.07	1.95	1.65	1.31	1.12	1.01	0.67	0.25
		ANN	1.32	1.73	2.07	1.95	1.65	1.31	1.12	1.01	0.66	0.25
	22	BNPPNA	0.73	0.95	1.14	1.07	0.91	0.72	0.62	0.55	0.37	0.14
		ANN	0.73	0.95	1.14	1.07	0.91	0.72	0.62	0.55	0.36	0.14
	23	BNPPNA	0.72	0.94	1.14	1.07	0.91	0.72	0.62	0.56	0.37	0.14
		ANN	0.72	0.94	1.14	1.07	0.91	0.72	0.62	0.56	0.37	0.14
	24	BNPPNA	0.75	0.97	1.17	1.10	0.93	0.74	0.63	0.57	0.38	0.14
		ANN	0.75	0.95	1.17	1.11	0.93	0.74	0.63	0.54	0.38	0.13
	25	BNPPNA	0.80	1.04	1.25	1.18	1.00	0.76	0.68	0.64	0.40	0.15
		ANN	0.80	1.04	1.25	1.18	1.02	0.76	0.68	0.64	0.40	0.15
	26	BNPPNA	0.85	1.14	1.36	1.28	1.06	0.86	0.73	0.56	0.44	0.44
		ANN	0.85	1.14	1.36	1.28	1.06	0.86	0.73	0.56	0.44	0.44
	27	BNPPNA	1.43	1.83	2.23	2.12	1.78	1.48	1.21	1.04	0.72	0.26
		ANN	1.43	1.83	2.23	2.12	1.78	1.48	1.21	1.04	0.70	0.26
	28	BNPPNA	1.41	1.83	2.20	2.07	1.75	1.39	1.19	1.07	0.71	0.24
		ANN	1.40	1.83	2.21	2.07	1.75	1.39	1.19	1.06	0.71	0.24

shows the axial RPD prediction in FA number 27 where the PPF is occurred.

The error values of radial RPD prediction by ANN for each FA in 1/6 core are shown in Fig. 12 for all cases given in Table 7. The average error of Case 1 to 5 are 0.99%, 0.22%, 0.14%, 0.93% and 0.36%, respectively.

7. Conclusion

This paper introduced a new tool for RPD and PPF predictions in a VVER reactor core based on an ANN framework and a series of experimental and calculated reactor operation data that were used for network training, validation and testing to develop an accurate monitoring system which can be incorporated into the reactor protection system. MLP networks with different number of hidden layers and various number of neurons in each layer were examined for this application. Based on the results, an MLP network with two hidden layers was chosen. The performance of proposed ANN was evaluated by MSE calculation and regression plot which indicated an average MSE less than 0.6 percent and an R value greater than 0.99. Besides, the error aggregation was observed to occur around the minimum error which is a criterion for a neural network with efficient performance. Also, investigation of different core parameters used in training process showed that the RPD variation is extremely sensitive to the position of control rods groups and the signal of ex-core neutron detector. The results proved the necessity

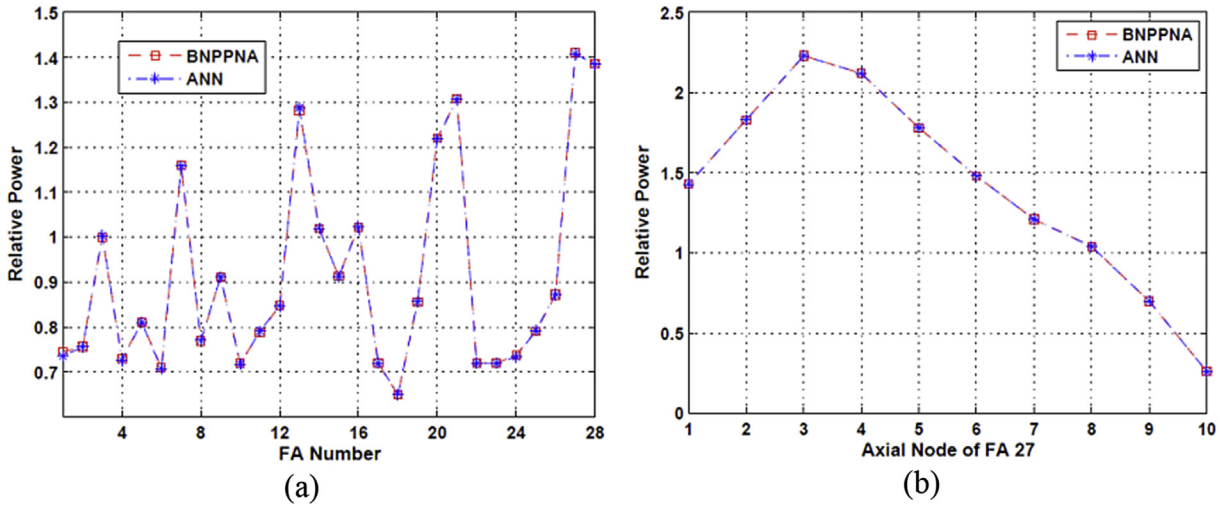

Fig. 11. ANN prediction results for Case 2 compared to BNPPNA data (a) radial RPD and (b) axial RPD in FA number 27.

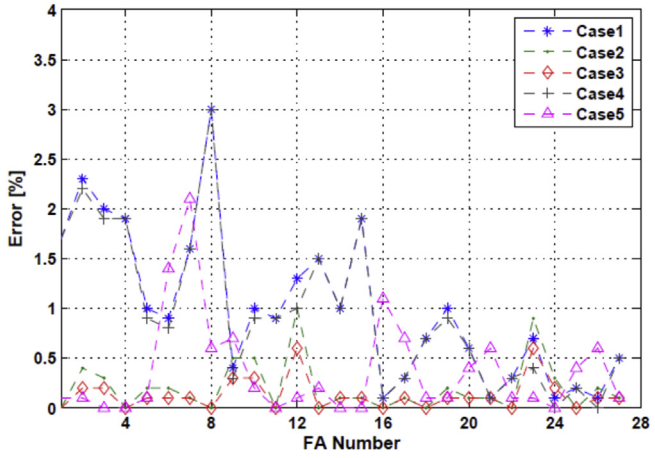

Fig. 12. Prediction error of radial RPD for each FA in 1/6 core for all reactor operation states given in Table 7.

of ex-core detector signals application for an accurate and reliable estimation of radial and axial RPDs and PPF using ANNs. Furthermore, the ability of MLP network in real-time prediction of RPD and PPF was assessed for various practical core states which were not used in training, validation, and testing processes. The results verified the capability and high accuracy of the proposed MLP network in RPD and PPF predictions.

References

Atomic Energy Organization of Iran (AEOI), 2007. BUSHEHR Nuclear Power Plant FSAR (Chapter 7): Instrumentation and control systems (I&C), Book1.

Atomic Energy Organization of Iran (AEOI), 2004. Album of Neutron and Physical Characteristics of the 1-st Loading of BNPP. Organization of Activities on BNPP-1Commissioning.

Bae, I.H., Gyun, M., Lee, Y.J., Park, G.C., 2009. Estimation of the power peking factor in nuclear reactor using support vector machine. Nucl. Eng. Technol. 41, 1181–1190.

Beale, M.H., Hagan, M.T., Demuth, H.B., 2014. Neural Network Toolbox User's Guide. Math Works Inc.

Briemeister, J.F., 2013. MCNPX a General Monte Carlo N-particle Transport Code, Version X.2.7. Los Alamos National Laboratory. La-13709.

Brown, F.B., 2000. The Makxsf Code with Doppler Broadening, X-3 Monte Carlo Codes. Los Alamos National Laboratory.

Dunn, W.L., Shultis, J.K., 2011. Exploring Monte Carlo Methods, first ed. Elsevier.

Hadad, K., Piroozmand, A., 2007. Application of cellular neural network (CNN) method to the nuclear reactor dynamics equations. Ann. Nucl. Energy 34, 406–416.

Hassoun, M., 2003. Fundamentals of Artificial Neural Networks. A Bradford Book.

International Atomic Energy Agency, 2005. Design of the Reactor Core for Nuclear Power Plants. IAEA Safety Standards, IAEA Publication.

Mary, R., Souza, G.P., Moreira, M.L., 2006. Neural network correlation for power peaking factor estimation. Ann. Nucl. Energy 33, 594–608.

Montes, J.L., Francois, J., 2009. Local power peaking factor estimation in nuclear fuel by artificial neural networks. Ann. Nucl. Energy 36, 121–130.

Nae, M., Jung, D.W., Shin, S.H., 2004. Estimation of the nuclear power peaking factor using in-core sensor signals. J. Korean Nucl. Soc. 36, 420–429.

Pirouzmand, A., Ghasemi, A., Faghihi, F., 2014. Safety analysis of LBLOCA with station blackout for the BUSHEHR's VVER-1000 nuclear power plant. In: Nurer2014 Conference, Antalya, Turkey.

Pirouzmand, A., Hadad, K., 2011. Cellular neural network to the spherical harmonics approximation of neutron transport equation in x–y geometry part I: modeling and verification for time-independent solution. Ann. Nucl. Energy 47, 225–233.

Pirouzmand, A., Hadad, K., Suh, K.Y., 2011b. Analog computing for a new nuclear reactor dynamic model based on a time-dependent second order form of the neutron transport equation. Nucl. Eng. Technol. 43, 243–256.

Tanabe, A., Yamamoto, T., 1993. Development of neural network for analysis of local power distributions in bare fuel bundles. Nucl. Sci. Tech. 30, 804–812.

Wang, Y., Zhengpei, F.L., Han, S., 2003. On-line monitoring the in-core power distribution by using ex-core ion-chambers. Nucl. Eng. Des. 225, 315–326.

Xia, J., Li, B., Liu, J., 2013. Research on intelligent monitor for 3D power distribution of reactor Core. Ann. Nucl. Energy 73, 446–454.